

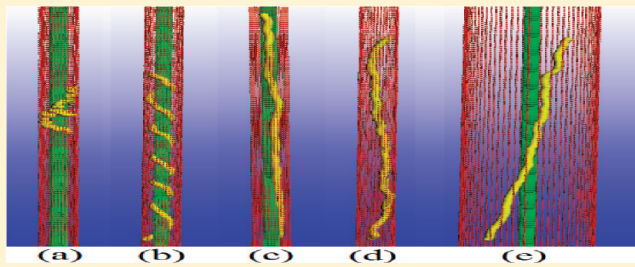
Helical Conformations of Semiflexible Polymers Confined between Two Concentric Cylinders

Dong Zhang,[†] Zhiyong Yang,[†] Xiaohui Wen,[†] Zhangheng Xiang,[†] Linli He,[‡] Shiyong Ran,[‡] and Linxi Zhang^{*,‡}

[†]Department of Physics, Zhejiang University, Hangzhou 310027, China

[‡]Department of Physics, Wenzhou University, Wenzhou 325035, China

ABSTRACT: An off-lattice Monte Carlo method was used to study the conformational properties of semiflexible chains confined between two concentric cylinders. The conformations of confined semiflexible chains depend on the bending energy as well as the size of confinement, and the semiflexible chains with particular rigidities confined in the appropriate spaces can form helical structures under entropically driven. The inner cylinder plays a key role in the formation of helical conformations, whereas the outer cylinder affects the size of confinement. Furthermore, the helical structures keep fluctuating like a harmonic oscillation, and the clockwise or counterclockwise helical conformations will appear with the same possibility in the processes of relaxation–helix transitions. This study can help us understand the conformational behaviors of biological macromolecules in confined space.



1. INTRODUCTION

The conformational properties of biomolecules are important for their functionality. For DNA, transcription and replication are governed by specific binding of proteins, and the mechanism is strongly connected to molecular configuration.^{1,2} Furthermore, conformational transitions of cytoskeletal filaments represent small engines,³ an idea that might be transferable to building biomimetic nanoactuators. On the other hand, the rigidity of biomolecule also has an important impact on its biological function.⁴ For example, the flexibility of DNA can allow it to effectively store and transfer a large amount of genetic information in a narrow space, whereas the semiflexible and rigid molecules are closely related to the mechanical properties of cells.^{5,6} Recently, the confined semiflexible polymer has attracted a lot of attention because a huge number of biomolecules crucial to life are constrained in narrow volumes *in vivo*. For example, the genome is highly confined spatially in living organisms, at all levels of complexity.⁷ And numerous important biological processes and technological applications also occur in a confined environment, such as the packaging of DNA or RNA in a virus⁸ and the packaging of DNA in eukaryotic cells,⁹ where, in both cases, the radius of gyration for the confined genome is much less than that of the unconfined. Additionally, confinements of polymers are encountered in large numbers of applications, such as filtration, colloidal stabilization,¹⁰ flow-injection problems,¹¹ and drug-delivery techniques.¹²

The helical structure is a recurring ordered chiral structure that exists in many biological molecules. Apart from some synthetic polymers,¹³ the biological polymers can also form a helix, such as ds-DNA and actin filaments, which spontaneously develop a helical conformation due to its inherent chemical structure.⁴ Snir et al. have discovered that the tube polymers immersed in a

solution of hard spheres can form the helix under entropically driven.^{14,15} The tube polymers mean that the polymers are modeled as the solid and impenetrable tubes, and in fact, the tube polymers can be regarded as the semiflexible chains with a large overlap excluded volume.^{14,15} And the formations of helical structures for semiflexible or stiff polymers have been found when they are bound to a cylinder surface,^{16–18} circle around attractive inner surface of a sphere,¹⁹ wrap around attractive outer surface of a sphere,²⁰ and confine in the ribosome exit tunnel.²¹ However, the studies about the conformations of semiflexible polymer chains in the different confinements are rare. Vogel et al. investigated conformational behaviors of polymers adsorbed at an attractive stringlike nanowire, and some important results such as compact droplets attached to the wire and nanotubelike monolayer films wrapping in a very ordered way are found.²² Yang et al. discussed the free energy and extension of semiflexible polymers in cylindrical confining geometries and their results are relevant for interpreting experiments on biopolymers in microchannel or microfluidic devices.²³ Recently, we have found that the semiflexible polymers confined in spheres can form local helical structures.²⁴ And much more works have been done to explore the conformations of chains confined in different environments. In fact, the shape of confined space plays a key role in the formation of helical conformation for semiflexible polymer chains.

There are two common kinds of confinements: film and porous media, which correspond to the flat boundary and the curved boundary cases, respectively.²⁵ This kind of confinement

Received: May 21, 2011

Revised: October 18, 2011

Published: October 19, 2011

can reduce to the one in a cylindrical pore or the one confined between two slabs, ultimately.²⁵ In reality, such system can be met in the case of film-coating on a cylindrical substrate.^{26,27} In this paper, by employing dynamic Monte Carlo simulation,²⁸ we have studied the conformational behaviors of semiflexible chains confined between two concentric cylinders. The helical conformations of polymer chains with the particular rigidities confined in the appropriate space are observed, and this study can help us understand the conformational behaviors of biological macromolecules in confinements.

2. SIMULATION MODEL AND METHOD

The semiflexible polymer chains are confined between two concentric cylinders with the inner radius R_1 and the outer radius R_2 , whereas the two concentric cylinders are infinite and impenetrable. There is no interaction between the polymer chains and the cylinders. To describe the dynamic behaviors of the polymer chains, we employ the dynamic Monte Carlo simulation, which is based on three-dimensional off-lattice bead–spring model. This method is always used for the simulations of polymers both in the bulk and in the confined environments.^{21,29}

The polymer chain contains N monomers and the neighbors are connected by the finitely extendible nonlinear elastic (FENE) potential³⁰

$$U_{\text{FENE}} = \sum -\kappa r'^2 \ln \left[1 - \left(\frac{l_i - l_0}{r'} \right)^2 \right] \quad (1)$$

Here l_i is the length of an effective bond, which ranges from $l_{\min} = 0.4$ to $l_{\max} = 1.0$ (l_{\max} is chosen to be the unit of length), and $l_0 = 0.7$ is the preferred distance, $r' = l_{\max} - l_0 = l_0 - l_{\min}$, the spring constant κ is set to 20 in the unit of $k_B T$.

A Morse-type potential is used for all nonbonded monomers which have excluded volume interaction, this potential includes a quasi-hard-core self-avoidance and an attractive part³⁰

$$U_{\text{Morse}} = \sum_{\substack{i=1 \\ j > i}}^N \varepsilon \{ \exp[-2\alpha(r_{ij} - r_{\min})] - 2 \exp[-\alpha(r_{ij} - r_{\min})] \} \quad (2)$$

Here r_{ij} is the distance between the i th and j th monomers, and $\varepsilon = 1.0$, $\alpha = 24$, $r_{\min} = 0.8$ are selected. The combination of FENE bonds and Morse potentials can prevent the unphysical crossing of chain.

The stiffness of the semiflexible polymer chains is described by the bending potential³⁰

$$U_{\text{bend}} = \sum_{i=2}^{N-1} b(1 + \cos \theta_i) \quad (3)$$

Here θ_i is the bond angle and b is the bending energy.

The total energy of the polymer chain can be written as

$$U = U_{\text{FENE}} + U_{\text{Morse}} + U_{\text{bend}} \quad (4)$$

Here, the employed simulation method is the off-lattice Monte Carlo algorithm. The initial configurations are generated randomly, and most of them are coil. In fact, a very long relaxation time (at last 2×10^9 MCSs) is needed for polymers to reach the equilibration states, and the initial configurations do not affect their ultimate results. To relax the polymer chain between the

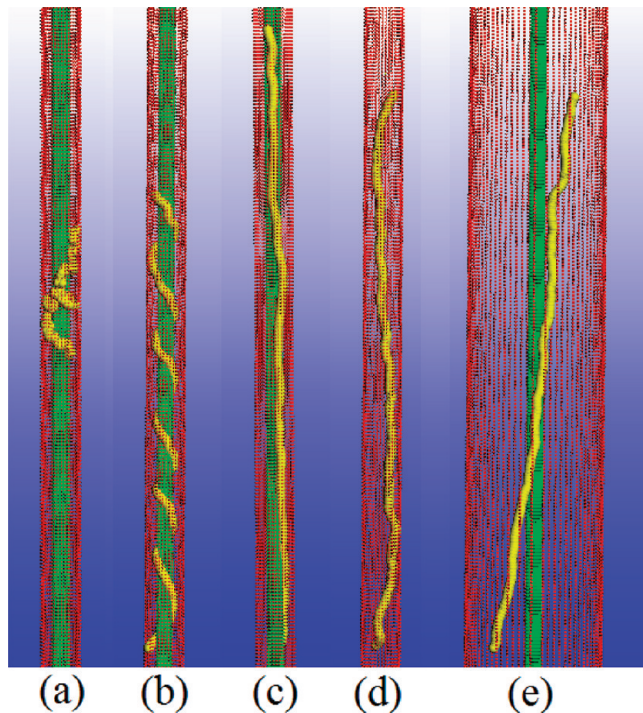


Figure 1. Snapshots for the 200-monomer chains with various rigidities confined between different concentric cylinders: (a) $R_1 = 2$, $R_2 = 5$, $b = 0$; (b) $R_1 = 2$, $R_2 = 5$, $b = 20$; (c) $R_1 = 2$, $R_2 = 5$, $b = 200$; (d) $R_1 = 0$, $R_2 = 5$, $b = 20$; (e) $R_1 = 2$, $R_2 = 20$, $b = 20$.

concentric cylinders, a randomly selected monomer is displaced from its position (x, y, z) to a new position (x', y', z') ,^{24,31} and increments $\Delta x = x' - x$, $\Delta y = y' - y$, $\Delta z = z' - z$ are chosen randomly from the intervals of $-0.2 \leq \Delta x, \Delta y, \Delta z \leq 0.2$. And if the displacement leads to violate bond-length restriction or overlap, the movement is rejected; otherwise, the acceptance of the displacement is evaluated by the Metropolis algorithm³² with the statistical weight $\exp(-\Delta U/k_B T)$, where ΔU is the total energy difference between the new and old configurations. Such Monte Carlo algorithms based on local moves of the monomers realize dynamics for the polymer chain.²⁸ To ensure equilibration, about 2×10^9 MCSs are performed prior to calculating average properties. A Monte Carlo step (MCS) is defined as the attempted movements for all monomers of the polymer chain. The data are collected by averaging over 100 independent runs, and each independent run includes 500 measurements at intervals of 5×10^6 MCSs. Therefore, the statistical quantities of confined polymer chains are averaged over 50 000 samples, and the errors of ensemble averages are controlled in the reasonable range.

3. RESULTS AND DISCUSSION

3.1. Helical Conformations of Confined Semiflexible Chains. The inner and outer radii of the concentric cylinders and the rigidity of polymer chains play key roles on the conformations of the confined chain. Figure 1 shows the simulation snapshots of the semiflexible chains with various rigidities confined between different concentric cylinders for chain length $N = 200$ monomers. Here the initial conformations in Figure 1 are all the coils. For the flexible chain ($b = 0$), the confined conformation is coil and disordered, as shown in Figure 1a. When the bending energy increases to $b = 20$, there

is an obvious helical conformation along the z -axis (Figure 1b). When the bending energy increases to $b = 200$ further, the helical conformation is destroyed and the confined chains become rod-like (Figure 1c). When the inner radius of the concentric cylinders decreases or the outer radius of the concentric cylinders increases further, the helical conformations completely disappear and the polymer chains become rod-like structures, as shown in Figure 1d,e, respectively. For the same confinement, the conformations of confined polymers also depend on the bending energy b . The bending strength $b = 20$ can be discussed by comparing with the Morse interaction strength between monomers. For example, when the distance between the i th and j th monomers decreases from $r_{ij} = 0.8$ to $r_{ij} = 0.76$ by 5%, the change in the Morse energy is $\Delta U_{\text{Morse}} = U_{\text{Morse}}(r_{ij}=0.76) - U_{\text{Morse}}(r_{ij}=0.80) = 2.60$, and the Morse potential is repulsive because of $\Delta U_{\text{Morse}} > 0$. At the same time, the average bond angle of a 200-monomer polymer is $\langle \theta \rangle = 164.3^\circ$ for $b = 20$, and when the bond angle decreases from $\theta = 164.3^\circ$ to $\theta = 156.1^\circ$ by 5%, the change in the bending energy is $\Delta U_{\text{bend}} = U_{\text{bend}}(\theta=156.1^\circ) - U_{\text{bend}}(\theta=164.3^\circ) = 0.97$, which is only one-third of the Morse energy change. In fact, the bond angle depends mainly on the bending potential, i.e., the value of b . For example, when the value of b increases from $b = 0$ to $b = 20$, the average bond angle increases from $\langle \theta \rangle = 103.6^\circ$ to $\langle \theta \rangle = 164.3^\circ$, and the average bond angle becomes $\langle \theta \rangle = 172.7^\circ$ for $b = 100$ and $N = 200$. In Figure 1b, the helical structure is very ordered, and the bending potential can preclude situations when a kink separates two portions of a chain (two helices) that wind in the opposite direction because a large bending energy is needed for the case that the helices wind in the opposite direction. Obviously, if the bending energy is low and the overlap excluded volume is large, two portions of a chain (two helices) can wind in the opposite direction.^{14,15} Combined with the results in ref 33, we find that the effect of confinement is similar to a weak attractive potential field between the polymer chains and the inner cylinder. It is the interplay of the bending energy and entropy that govern the equilibrium conformations of the polymer chains. The equilibrium conformation is controlled by the rigidity of the polymer chain and the size of confined space.^{34,35} And their competition determines the equilibrium conformations.

To quantitatively distinguish between helical periodicity and coil, a spatial correlation function has been used³⁶

$$G(m) = \frac{1}{N-3} \sum_{i=2}^{N-2} g(m, i) \quad (5)$$

Here N is the number of monomers in the polymer chain, m means sequence interval, which ranges from 0 to $N/2 - 1$. And $g(m, i)$ is given by³⁶

$$g(m, i) = \frac{1/(N-m-1) \sum_{j=1}^{N-m-1} (\cos \theta_{ij} - \overline{\cos \theta_{ij}})(\cos \theta_{i,j+m} - \overline{\cos \theta_{ij}})}{1/(N-1) \sum_{j=1}^{N-1} (\cos \theta_{ij} - \overline{\cos \theta_{ij}})^2} \quad (6)$$

The angle θ_{ij} is defined as

$$\cos \theta_{ij} = \frac{\vec{l}_i \cdot \vec{l}_j}{|\vec{l}_i| |\vec{l}_j|} \quad (7)$$

Here $\vec{l}_i = \vec{r}_{i+1} - \vec{r}_i$ is the i th bond vector, and $\overline{\cos \theta_{ij}}$ denotes the average of $\cos \theta_{ij}$ over j from 1 to $N - 1$.

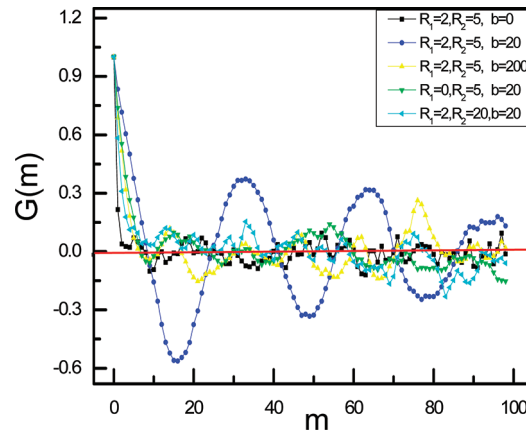


Figure 2. Spatial correlation function $G(m)$ of confined chains for the five conformations in Figure 1, respectively.

The values of $G(m)$ for a series of sequence interval can be fitted by the following empirical equation:³⁶

$$G(m) = \exp(-m/\xi) \cos(2\pi m/P) \quad (8)$$

Here, two parameters, ξ and P , are interpreted as the orientational correlation length and period of helix, respectively. P is equivalent to the average number of monomers per turn of the analyzed chains; ξ describes the correlation of monomers along the chain contour. For a perfect helix, ξ tends to be infinity, and the exponential decay with no oscillations would be observed for nonperiodic conformations.³⁷

The values of $G(m)$ for five conformations in Figure 1 have been shown in Figure 2, and they provide further evidence for helical conformations of the confined chains with the appropriate bending energy and size of confined space. For the helical conformation with $R_1 = 2$, $R_2 = 5$, and $b = 20$, the average number of monomers in one helical period is $P = 32$, and the average orientational correlation length of monomers along the chain contour is $\xi = 42$. Therefore, in our simulation, the average helix pitch is long and the number of monomers in one helical period is large. Simultaneously, the correlation function $G(m)$ is randomly oscillating and the helical conformation is not exactly periodic for other cases in Figure 2.

To determine the helical conformations in more detail, the combination of $\cos(\phi_i)$ and $\cos(\varphi_i)$ are used, as shown in Figure 3, respectively. Because the concentric cylinders are infinite and the helical conformation is along z -axis direction, the fluctuations of confined chains along the z -axis affect the helical conformations; therefore, we only discuss the conformations of confined chains in the xy -plane. We define $\cos(\phi_i)$ and $\cos(\varphi_i)$ as

$$\cos(\phi_i) = \frac{\vec{b}_i \cdot \vec{b}_0}{|\vec{b}_i|} \quad (9)$$

$$\cos(\varphi_i) = \frac{\vec{u}_i \cdot \vec{u}_1}{|\vec{u}_i| |\vec{u}_1|} \quad (10)$$

Here $\vec{b}_i = \vec{r}_{i+1}' - \vec{r}_i'$, $\vec{u}_i = \vec{r}_{i+1}' - \vec{r}_i'$, and $\vec{r}_i' = (x_i, y_i)$ is the projection of i th bond vector on the xy -plane, and $\vec{b}_0 = (1, 0)$ is a constant vector.

Comparing Figures 1 and 3, we can observe that $\cos(\phi_i)$ and $\cos(\varphi_i)$ oscillate uniformly for the helical structure, and they are

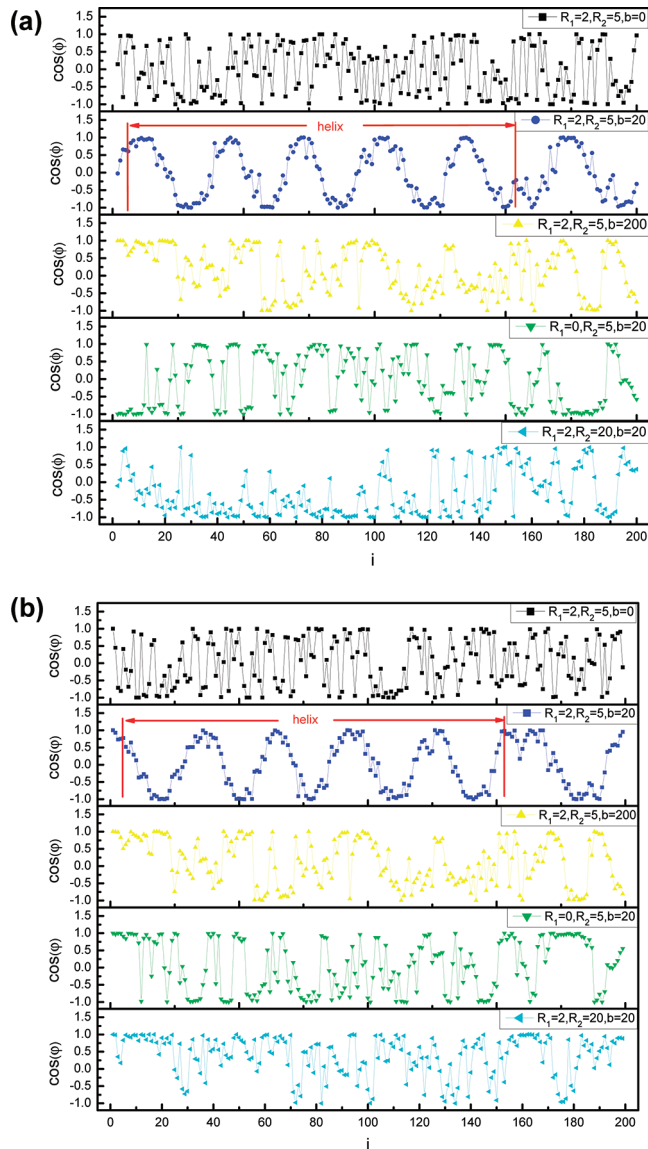


Figure 3. (a) $\cos(\phi)$ and (b) the $\cos(\phi)$ as a function of monomer i for five conformations in Figure 1, respectively.

disordered for improper stiffness of the chain or large size of the confined space. On the other hand, for the system with $R_1 = 2$, $R_2 = 5$, and $b = 20$, the number of periods in the periodic uniform oscillation of $\cos(\phi_i)$ and $\cos(\varphi_i)$ corresponds to the number of helix turns in Figure 1b. Therefore, through calculating the values of $\cos(\phi_i)$ and $\cos(\varphi_i)$, we can obtain the statistical properties of helical conformations, such as the average helix content and the average number of helical turns.

3.2. Statistical Properties of Confined Semiflexible Chains.

To explore the conformations of confined chains further, we calculate the average helix contents P_h and the average helical turns N_h as a function of the bending energy b for different confined systems, and the results are shown in Figure 4, respectively. Here $P_h \equiv (1/M)\sum_{i=1}^M (N_{\text{helix}}^i/N)$, and $N_h \equiv (1/M)\sum_{i=1}^M (N_{\text{helix}}^i/N_h^i)$, N_{helix}^i is the number of monomers of helix in the i th sample, N_h^i is the number of helical turns in the i th sample, M is the number of samples,²⁴ and $M = 5 \times 10^4$. When the 200-monomer polymer chains are confined between the concentric

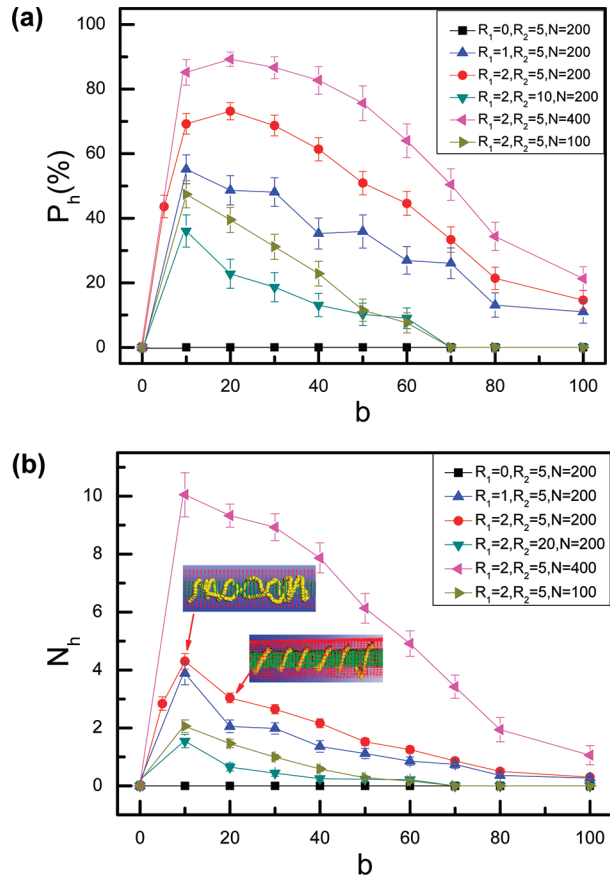


Figure 4. (a) Average percentage P_h of helix monomers in a chain and (b) the average helix turns N_h as a function of the bending energy b for confined chains with different concentric cylinders and chain lengths. Inset figures in Figure 4b show the possible helical conformations.

cylinders with $R_1 = 2$ and $R_2 = 5$, the helical conformations can be observed in a large range of bending energy b . The average helix contents P_h are very large and the value of P_h is about 60–70% in the range $b = 10$ to $b = 50$. It reaches the maximum $P_h = 73\%$ for the bending energy $b = 20$. Corresponding to P_h , the average helical turns N_h also increase when the bending energy increases from $b = 10$ to $b = 50$. There is a shape peak at $b = 10$ for N_h . As shown in the inset of Figure 4b, there are two different helical conformations at $b = 10$, i.e., single helix and double helix, whereas there is only the single helical conformation for $b \geq 20$. Because the bending energy $b = 10$ is low, the confined polymer chains can wrap back and form double helical conformations. And comparing to the single helix, the average helical turns for double helical conformations are large. Therefore, the average helical turns for $b = 10$ are larger than the others. The helical structures are affected by the bending energy b deeply. When the confined size is expanded to the outer radius $R_2 = 20$ or the inner radius $R_1 = 1$, the values of P_h and N_h are lower than those for $R_1 = 2$ and $R_2 = 5$ in the all ranges of bending energy b . And they reach the maximum at $b = 10$ and then decrease with the increases of bending energy b . The formation of helical conformations also depends on the size of confined space. On the other hand, the helical structure disappears completely when the inner radius decreases to zero, which reveals that the inner radius of the concentric cylinders also plays a key role in the formation of the helical conformations. At the same time, the chain length

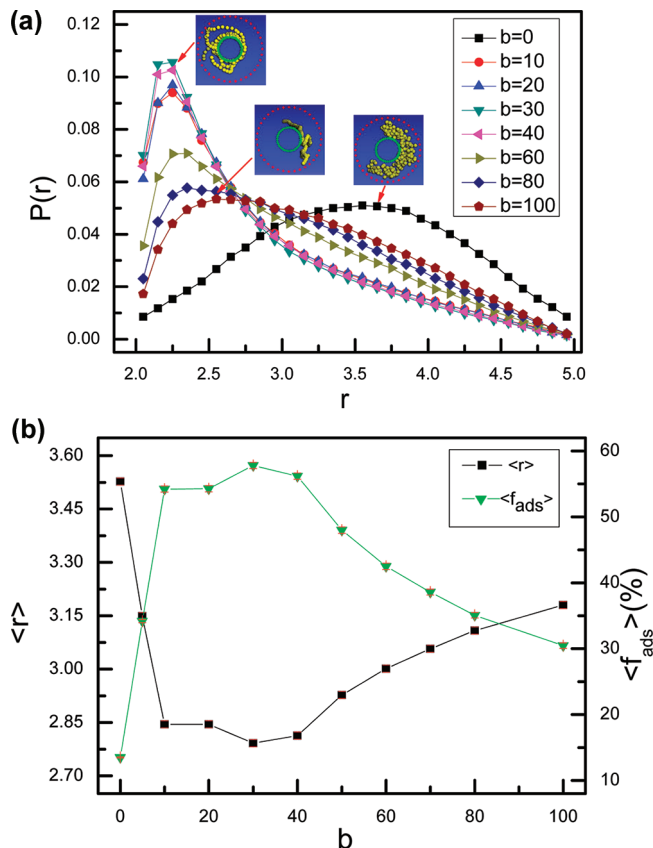


Figure 5. (a) Probability distribution $P(r)$ of monomers for confined chains with different rigidities $b = 0, 10, 20, 30, 40, 60, 80, and 100 . (b) The average distance $\langle r \rangle$ of confined chains to the z -axis (left) and the average absorbed fraction $\langle f_{\text{ads}} \rangle$ of confined chains (right) as a function of the bending energy b . Here the size of concentric cylinder is $R_1 = 2$ and $R_2 = 5$, chain length $N = 200$, and the inset figures show the possible conformations in the xy -plane.$

can also affect the helical structures deeply, and the results for different chain lengths ($N = 100$ and 400) are also given in Figure 4. The average helix contents P_h and the average helical turns N_h for $N = 400$ are larger than those for $N = 200$ in the all ranges of bending energy b at $R_1 = 2$ and $R_2 = 5$, and the short chain case ($N = 100$) is contrary. In other words, the longer the chain length of the polymer, the higher the helicity of the polymer.

Entropy can drive the confined semiflexible polymer chains to form helical structure.³⁸ Lue et al. have demonstrated that the delicate interplay between attractive interaction and packing (due to excluded volume interaction) of monomers can induce a helix.³⁹ The inner cylinder is necessary because it provides a very important intermedium for the formation of helical structure, as shown in Figure 1d. The inner radius will affect immediately the average helix content and the average helical turns of polymer chains, as shown in Figure 4a,b, respectively. To understand the effects of bending energy and confinement size on the polymer chain structures in more detail, we try to analyze them theoretically through the free energy F . As is known, the total change in free energy ΔF between the confined chains with helical structures (Figure 1b) and the confined chains with the rod-like (Figure 1c) or disordered structures (Figure 1a) can be written as $\Delta F = \Delta U - k_B T \Delta V_{\text{overlap}} - T \Delta S$, where ΔU , $\Delta V_{\text{overlap}}$ and ΔS are the changes of energy, total overlap excluded volume,

and conformational entropy, respectively.^{14,15,24} According to the thermodynamic conditions, the system will reach equilibrium along the direction of $\Delta F \leq 0$ spontaneously. For the flexible polymer with $b = 0$, the total change in free energy ΔF is almost equal to the change of conformational entropy,^{40,41} and therefore, the equilibrium conformation of $b = 0$ is a disordered coil (Figure 1a). When the bending energy $b \geq 200$, the change of energy ΔU dominates the change of total free energy ΔF , and therefore the equilibrium structure turns to the rod-like structure, as shown in Figure 1c. In another case, the large size of the confined space implies that the polymer chain can extend itself adequately and the total overlap volume $\Delta V_{\text{overlap}}$ will decrease deeply. Thus, there is no motivation for the confined chain to form helical structures, as shown in Figure 1e. In summary, only the appropriate ranges of bending energy and confined size can allow $k_B T \Delta V_{\text{overlap}} < \Delta U - T \Delta S$, which means that $\Delta F \leq 0$ is possible in the process of coil–helix transition.²⁴ In other words, particular values of b , R_1 , and R_2 can lead to the formation of helical conformations, as shown in Figure 1b.

The probability distributions $P(r)$ of monomers for the confined chains with different rigidities are shown in Figure 5a. Here $P(r)$ means the probability of finding a monomer in the interval of $[r, r + dr]$. The probability distribution of the flexible chains (i.e., $b = 0$) shows that the flexible chains would like to stay in the middle of the confined space and $P(r)$ reaches the maximum at $r = 3.5$. When the bending energy is in the range $b = 10–40$, $P(r)$ has a sharp peak at $r = 2.25$ and decreases rapidly for $r \geq 2.5$. The helical conformations are formed near the inner cylinder surface. When the bending energy b increases further, the helical conformations disappear gradually and the peak of $P(r)$ shifts to the large value of r slowly. At the same time, the height and width of the peak change significantly, which indicates that the polymer chains with large rigidities tend to stay away from the inner cylinder and distribute in a wide area. The projections of conformations on the xy -plane for $b = 0, 30$, and 100 have been shown in the inset of Figure 5a. Additionally, the average distance from the inner cylinder $\langle r \rangle$ for polymer chains and the average absorbed fractions $\langle f_{\text{ads}} \rangle$ of polymer chains as a function of the bending energy b for the system of $R_1 = 2$ and $R_2 = 5$ are shown in Figure 5b. Here the average absorbed fraction $\langle f_{\text{ads}} \rangle$ is defined as the percentage of the monomers near the inner cylinder surface (at a distance $D \leq 0.7$ from the inner cylinder cylinder).³⁵ At first, the average distance $\langle r \rangle$ (or the average absorbed fraction $\langle f_{\text{ads}} \rangle$) decreases (increases) quickly with the increases of b . When the bending energy ranges from $b = 10$ to $b = 40$, the average distance $\langle r \rangle$ and the average absorbed fraction $\langle f_{\text{ads}} \rangle$ remain unchanged with $\langle r \rangle = 2.8$ and $\langle f_{\text{ads}} \rangle = 55\%$, respectively. This result indicates further that the helical structures are formed near the inner cylinder surface. For the large bending energy $b \geq 60$, the polymer chains are away from the inner cylinder, and this lead to the increment of the average distance $\langle r \rangle$ and the decrement of the average absorbed fraction $\langle f_{\text{ads}} \rangle$.

As the energy fluctuation $\langle U^2 \rangle - \langle U \rangle^2$ is similar to the specific heat C_V , which is always used to study the helix–coil transition of homopolymer chains,^{42,43} we calculate the energy fluctuation with different bending energies b for the system of $R_1 = 2$, $R_2 = 5$, and $N = 200$, and the results are shown in Figure 6. The transition from coil to helical structures occurs with the increase of b , which is characterized by a shape peak at $b = 10$ in the fluctuation of the total energy U . By calculating the energy fluctuation of bond energy, Morse potential, and bending potential, we find that the total energy fluctuation depends mainly on the bending

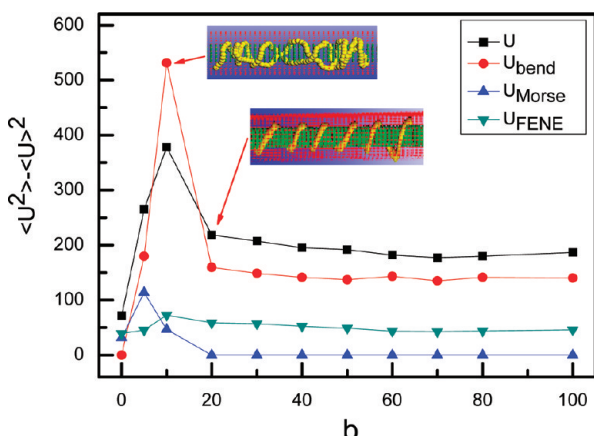


Figure 6. Energy fluctuations $\langle U^2 \rangle - \langle U \rangle^2$ as a function of the bending energy b for 200-monomer confined chains with the size of concentric cylinder $R_1 = 2$ and $R_2 = 5$. The insets show the possible helical conformations of confined with different rigidities.

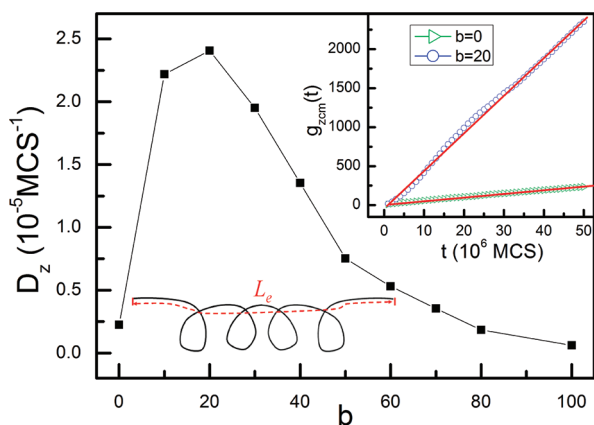


Figure 7. Diffusion coefficients in the z -direction D_z as a function of the bending energy b for confined semiflexible polymers. The inset shows the z -component of the center-of-mass autocorrelation function $g_{\text{zcm}}(t)$ as a function of simulation time t with different bending energies $b = 0$ and $b = 20$. Here $N = 200$, $R_1 = 2$, $R_2 = 5$, and L_e is the effective contour length of confined semiflexible polymers.

potential. For the bending energy $b < 20$, the combinations of U_{bend} , U_{Morse} , and U_{FENE} lead to the fluctuations of total energy, whereas for $b \geq 20$, only the U_{bend} and U_{FENE} can affect the total energy fluctuation. As we know, there are two different conformations (single helix and double helix) at $b = 10$ and the contribution of bending energy to the total energy fluctuation is very obvious, which has shown in the inset of Figure 6. Therefore, the fluctuations of the total energy and the bending energy are very remarkable for $b = 10$.

Additionally, we also study the diffusion behaviors of semiflexible polymers under the confinement by employing the z -component of the center-of-mass autocorrelation function $g_{\text{zcm}}(t)$, and the results are shown in Figure 7. $g_{\text{zcm}}(t)$ is defined as⁴⁴

$$g_{\text{zcm}}(t) = \langle |z_{\text{cm}}(t) - z_{\text{cm}}(0)|^2 \rangle \quad (11)$$

Here z_{cm} stands for the z -component of the center-of-mass coordinate. Though the dynamics of semiflexible polymers in solutions are rather different from the flexible polymers on short and medium time scales,^{45–48} the diffusion behaviors for the

confined semiflexible polymers on very long time scale satisfy $g_{\text{zcm}}(t) \sim t$ in our Monte Carlo simulation, and the results $g_{\text{zcm}}(t)$ as a function of time t for confined flexible polymer ($b = 0$) and semiflexible polymer (such as $b = 20$) are shown in the inset of Figure 7. The dynamics can be described by an exponent ν such that the center-of-mass displacement traveled in time varies asymptotically as $g_{\text{zcm}}(t) \sim t^\nu$. If $\nu = 1$, it is normal diffusion; otherwise, it is anomalous diffusion.^{48–50} The diffusion constant D_z of confined polymers along the z -direction is defined as

$$D_z = \lim_{t \rightarrow \infty} \frac{g_{\text{zcm}}(t)}{2t} \quad (12)$$

And the diffusion constant D_z of confined semiflexible polymers with different bending energies b are shown in Figure 7. Doi predicted that the diffusion constant is independent of bending energy when the stiffness of polymer chain is large enough,⁵¹ whereas Odijk concluded that the diffusion should be enhanced by flexibility,⁵² and those have been proved by Fakhri et al.⁵³ For semiflexible chains with contour length L , Odijk theory predicts that the diffusion constant should be

$$D^{\text{Odijk}} = \frac{k_B T}{\eta_0 L^2 L_p} = \frac{k_B^2 T^2}{\eta_0 L^2 b} \quad (13)$$

Here η_0 is the viscosity, $L_p = b/k_B T$ is the persistence length, and L is the contour length. If the confined semiflexible chains contain local helical structures, the contour length L may depend on the number of helical structures. Here we introduce a parameter L_e to describe the effective contour length of polymer chains (see the inset of Figure 7), and it should be more reasonable if L_e instead of L in eq 13. That is

$$D^{\text{Odijk}} = \frac{k_B T}{\eta_0 L_e^2 L_p} = \frac{k_B^2 T^2}{\eta_0 L_e^2 b} \quad (14)$$

In Figure 7, the diffusion constant D_z increases with the increase of the bending energy b for $b < 20$, and it decreases with the bending energy b for $b > 20$. This phenomenon can be explained in the qualitative trends according to Odijk theory, i.e., eq 14. When the bending energy b increases for small b , the average helix contents P_h also increases (Figure 4a), this leads to a decrease in the effective contour length L_e ; therefore, the diffusion constant D_z increases with the increase of the bending energy b , and it reaches a maximum at $b = 20$. When the bending energy b increases further, the helical structures will disappear gradually and the effective length L_e increases; therefore, the diffusion constant D_z decreases with the increase of the bending energy b . Therefore, the diffusion also depends on the bending energy b , and it reaches the maximum value at $b = 20$. Of course, the explanation based on Odijk theory is very approximate, and the description is qualitative rather than quantitative because the effective length L_e is vague. The dynamical behaviors for confined semiflexible polymers can help us understand the conformation properties of confined semiflexible in more detail

3.3. Helical Fluctuation and Clockwise–Counterclockwise Transition. In our simulations, there is no interaction between polymer chains and the inner cylinder surface. Thus, the helical structures are not stable and will be fluctuating in the simulation processes. Here the fluctuation means the process of helix–relaxation transition. Furthermore, the helical structures along the z -axis direction have two different conformations: clockwise helix and counterclockwise helix. To describe the orientation and

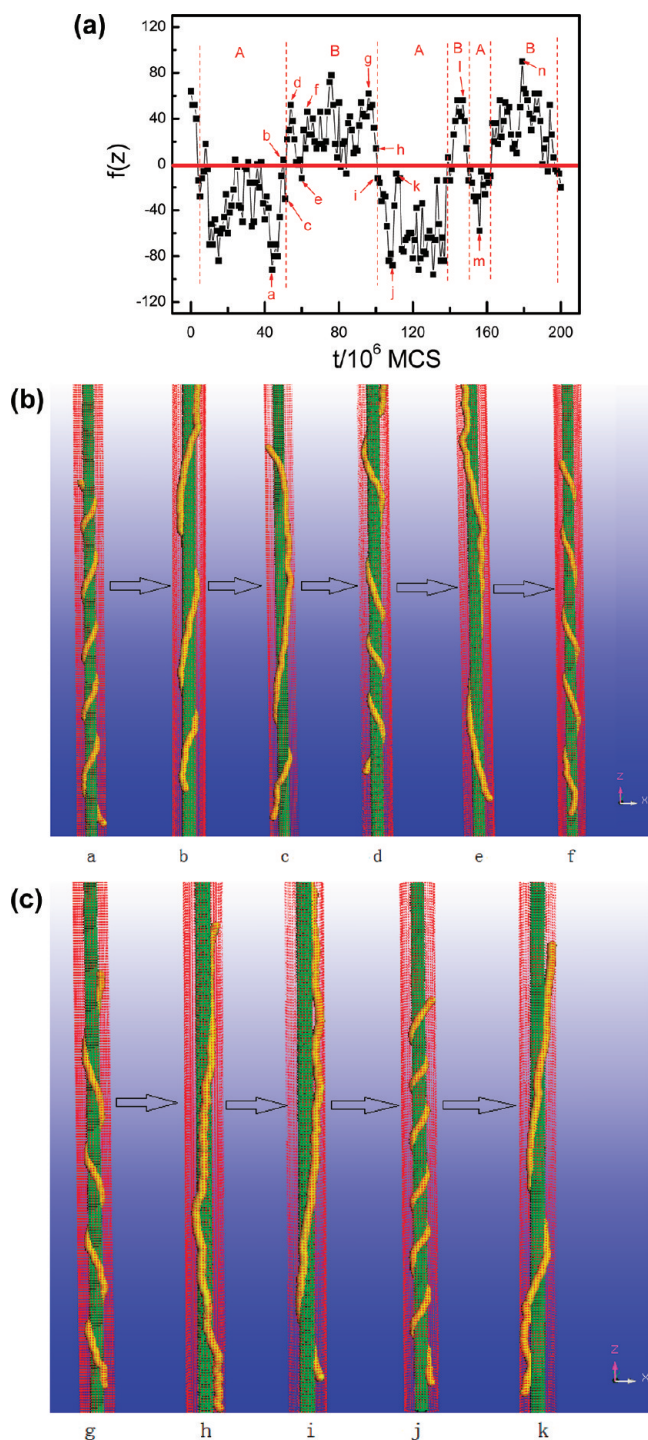


Figure 8. (a) Value of $f(z)$ as a function of simulation time t for confined chains with $R_1 = 2$, $R_2 = 5$, $b = 20$, and $N = 200$. (b) Simulation snapshots of the process $a \rightarrow b \rightarrow c \rightarrow d \rightarrow e \rightarrow f$. (c) Simulation snapshots of the process $g \rightarrow h \rightarrow i \rightarrow j \rightarrow k$.

the helicity of polymer chains, we define an expression $f(z)$ as

$$f(z) = - \sum_{i=2}^{N-1} \text{sgn}((\vec{l}_i \times \vec{l}_{i+1})_z) \quad (15)$$

Here $\vec{l}_i = \vec{r}_{i+1} - \vec{r}_i$ is the i th bond vector, subscript z means the z -component of vector, and $\text{sgn}(x)$ is a sign function, which is

defined as

$$\text{sgn}(x) = \begin{cases} 1 & x > 0 \\ 0 & x = 0 \\ -1 & x < 0 \end{cases} \quad (16)$$

If $f(z) < 0$, the orientation of the chain along z -axis is clockwise; otherwise, if $f(z) > 0$, the orientation is counterclockwise, and $f(z) = 0$ means the chain parallels to the z -axis roughly. Of course, the definition of $f(z)$ is only qualitatively correct because weakly and strongly helical parts of the chain would make the same contribution to $f(z)$. Roughly, the higher the helicity of polymer chain, the greater the magnitude of $f(z)$.

The value of $f(z)$ as a function of simulation time t for the system with $R_1 = 2$, $R_2 = 5$, $b = 20$, and $N = 200$ is shown in Figure 8a. According to the definition of $f(z)$, the fluctuation of $f(z)$ indicates the processes of helix–relaxation transitions and the oscillation of the sign of $f(z)$ means the processes of clockwise–counterclockwise helix transitions. Therefore, $f(z)$ can be separated into alternate parts by red dash as shown in Figure 8a. Part A means the conformations of polymer chains are clockwise helix, and part B means the conformations are counterclockwise helix. Obviously, a , j , and m have conformations similar to that of the maximum clockwise helix, whereas d , g , l , and n have conformations similar to that of the maximum counterclockwise helix. As representative examples, the simulation snapshots of the processes $a \rightarrow b \rightarrow c \rightarrow d \rightarrow e \rightarrow f$ and $g \rightarrow h \rightarrow i \rightarrow j \rightarrow k$ are shown in Figure 8b,c, respectively. In a general way, the well helical structure will relax to the rod-like one affected by perturbations and form a helix again under entropically driven.¹⁴ By analyzing the simulation snapshots and calculating the probability distributions, we find that the average widths of parts A and B are almost the same, which indicates that the clockwise and counterclockwise helical conformations will appear with the equal probability.

4. CONCLUSIONS

An off-lattice Monte Carlo algorithm has been used to study the semiflexible polymer chains confined between two concentric cylinders. An interesting result is that the particular confined chains can form helical structures under entropically driven conditions. First, the inner cylinder plays a key role in the formation of helical structures because it provides an intermedium for helix. And the size of the concentric cylinders will affect the features of helical conformations, such as the average helical contents and the average helical turns. The conformations of semiflexible chains depend on the bending energy and the size of concentric cylinders simultaneously. For the flexible polymer chain with $b = 0$, its conformation is coil, and for the rigid chain with $b \geq 200$ or the semiflexible chain confined in the large size space, it is rod-like. The helical structures can be formed only for the appropriate stiffness of semiflexible chains and the appropriate size of concentric cylinders. Finally, the helical structure is fluctuating because of the absence of interaction between the polymer chain and the inner cylinder surface, and the process of relaxation–helix transition is similar to the harmonic oscillation. At the same time, the clockwise and counterclockwise helical conformations along the z -axis will appear with the equal possibility. This study can help us understand how DNA chains fold in confined spaces, such as viruses and cells.

■ AUTHOR INFORMATION

Corresponding Author

*E-mail: lxzhang@zju.edu.cn.

■ ACKNOWLEDGMENT

This research was financially supported by the National Natural Science Foundation of China (Nos. 20974081, 20934004, 21174131, 21104060). We are also grateful to the reviewers of our manuscript for their detailed and insightful comments and suggestions.

■ REFERENCES

- (1) Gowers, D. M.; Halford, S. E. *EMBO J.* **2003**, *22*, 1410.
- (2) van den Broek, B.; Lomholt, M. A.; Kalisch, S. M. J.; Metzler, R.; Wuite, G. J. L. *Proc. Natl. Acad. Sci. U. S. A.* **2008**, *105*, 15738.
- (3) Schmid, M. F.; Sherman, M. B.; Matsudaira, P.; Chiu, W. *Nature* **2004**, *431*, 104.
- (4) Alberts, B.; Johnson, A.; Lewis, J.; Roberts, M. R. K. Walter, P. *Molecular Biology of a Cell*, 4th ed.; Garland: New York, 2002.
- (5) Howard, J. *Mechanics of Motor Proteins and the Cytoskeleton*; Sinauer: Sunderland, 2001.
- (6) Boal, D. *Mechanics of the Cell*; Cambridge University Press: Cambridge, U.K., 2002.
- (7) Marenduzzo, D.; Micheletti, C.; Orlandini, E. *J. Phys.: Condens. Matter* **2010**, *22*, 283102.
- (8) Lewin, B. *Genes VII*; Oxford University Press, New York, 2000.
- (9) Lodish, H.; Berk, A.; Zipursky, S. L.; Matsudaira, P.; Baltimore, D.; Darnell, J. *Molecular and Cellular Biology*; W. H. Freeman and Co.: San Francisco, 2000.
- (10) Hunter, R. J. *Foundations of Colloid Science*, 2nd ed.; Oxford University Press: Oxford, U.K., 2001.
- (11) Sakae, T.; Raphaël, E.; de Gennes, P. G.; Brochard-Wyart, F. *Eur. Phys. Lett.* **2005**, *72*, 83.
- (12) Gregoriadis, G. *Trends Biotechnol.* **1995**, *13*, 527.
- (13) Nakano, T.; Okamoto, Y. *Chem. Rev.* **2001**, *101*, 4013.
- (14) Snir, Y.; Kamien, R. D. *Science* **2005**, *307*, 1067.
- (15) Snir, Y.; Kamien, R. D. *Phys. Rev. E* **2007**, *75*, 05114.
- (16) Zheng, M.; Jagota, A.; Semke, E. D.; Diner, B. A.; Richardson, R. E.; Tassi, N. G. *Nat. Mater.* **2003**, *2*, 338.
- (17) Šarić, A.; Pàmies, J. C.; Cacciuto, A. *Phys. Rev. Lett.* **2010**, *104*, 226101.
- (18) Gurevitch, I.; Srebnik, S. *J. Chem. Phys.* **2008**, *128*, 144901.
- (19) Morrison, G.; Thirumalai, D. *Phys. Rev. E* **2009**, *79*, 011924.
- (20) Angelescu, D. G.; Linse, P.; Nguyen, T. T.; Bruinsma, R. F. *Eur. Phys. J. E* **2008**, *25*, 323.
- (21) Ziv, G.; Haran, G.; Thirumalai, D. *Proc. Natl. Acad. Sci. U. S. A.* **2005**, *102*, 18956.
- (22) Vogel, T.; Bachmann, M. *Phys. Rev. Lett.* **2010**, *104*, 198302.
- (23) Yang, Y. Z.; Burkhardt, T. W.; Gompper, G. *Phys. Rev. E* **2007**, *76*, 011804.
- (24) Yang, Y. Z.; Zhang, D.; Zhang, L. X.; Chen, H. P.; Rehman, A.; Liang, H. J. *Soft Matter* **2011**, *7*, 6836.
- (25) Suo, T.; Yan, D. *Polymer* **2011**, *52*, 1686.
- (26) Li, B.; Li, Y.; Xu, G. K.; Feng, X. Q. *J. Phys.: Condens. Matter* **2009**, *21*, 445006.
- (27) Lee, H. B.; Wuu, D. S.; Lee, C. Y.; Lin, C. S. *Tribol. Int.* **2010**, *43*, 235.
- (28) Milchev, A.; Binder, K.; Bhattacharya, A. *J. Chem. Phys.* **2004**, *121*, 6024.
- (29) Binder, K.; Milchev, A. *J. Comput.-Aided Mater. Des.* **2002**, *9*, 33.
- (30) Cifra, P. *J. Chem. Phys.* **2009**, *131*, 224903.
- (31) Avramova, K.; Milchev, A. *J. Chem. Phys.* **2006**, *124*, 024909.
- (32) Metropolis, N.; Rosenbluth, A. W.; Rosenbluth, M. N.; Teller, A. H.; Teller, E. *J. Chem. Phys.* **1953**, *21*, 1087.
- (33) Kusner, I.; Srebnik, S. *Chem. Phys. Lett.* **2006**, *430*, 84.
- (34) Burkhardt, T. W. *J. Phys. A* **1997**, *30*, L167.
- (35) Odijk, T. *Macromolecules* **1993**, *26*, 6897.
- (36) Chen, Y. Y.; Zhang, Q.; Ding, J. D. *J. Chem. Phys.* **2006**, *124*, 184903.
- (37) Gurevitch, I.; Srebnik, S. *Chem. Phys. Lett.* **2007**, *444*, 96.
- (38) Han, Y.; Zhao, L.; Ying, J. Y. *Adv. Matter* **2007**, *19*, 2454.
- (39) Magee, J. E.; Vasquez, V. R.; Lue, L. *Phys. Rev. Lett.* **2006**, *96*, 207802.
- (40) Lamura, A.; Burkhardt, T. W.; Gompper, G. *Phys. Rev. E* **2004**, *70*, 051804.
- (41) Nowicki, W.; Nowicka, G.; Michalek, J. N. *Eur. Polym. J.* **2010**, *46*, 112.
- (42) Su, J. Y.; Zhang, L. X.; Liang, H. J. *J. Chem. Phys.* **2008**, *129*, 044905.
- (43) Zhou, Y.; Hall, C. K.; Karplus, M. *Phys. Rev. Lett.* **1996**, *77*, 2822.
- (44) Muthukumar, M. *Macromolecules* **1989**, *22*, 1937.
- (45) Yamakov, V.; Stauffer, D.; Milchev, A.; Foo, G. M.; Pandey, R. B. *Phys. Rev. Lett.* **1997**, *79*, 2356.
- (46) Bohbot-Raviv, Y.; Zhao, W. Z.; Feingold, M.; Wiggins, C. H.; Granek, R. *Phys. Rev. Lett.* **2004**, *92*, 098101.
- (47) Goff, L.; Le, H.; Hallatschek, O.; Frey, E.; Amblard, F. *Phys. Rev. Lett.* **2002**, *89*, 258101.
- (48) Liverpool, T. B.; Maggs, A. C. *Macromolecules* **2001**, *34*, 6064.
- (49) Romiszowski, P.; Sikorski, A. *J. Chem. Phys.* **2002**, *116*, 4.
- (50) Sikorski, A.; Romiszowski, P. *J. Chem. Phys.* **1998**, *109*, 2912.
- (51) Doi, M. *J. Phys. (Paris)* **1975**, *36*, 607.
- (52) Odijk, T. *Macromolecules* **1983**, *16*, 1340.
- (53) Fakhri, N.; MacKintosh, F. C.; Lounis, B.; Cognet, L.; Pasquali, M. *Science* **2010**, *330*, 1804.